Journal of Magnetic Resonance 211 (2011) 18–24

Contents lists available at ScienceDirect

Journal of Magnetic Resonance

journal homepage: www.elsevier.com/locate/jmr

Frequency-selective heteronuclear dephasing and selective carbonyl labeling to deconvolute crowded spectra of membrane proteins by magic angle spinning NMR

Nathaniel J. Traaseth [a], Gianluigi Veglia [a,b,*]

[a] Department of Biochemistry, Molecular Biology, and Biophysics, University of Minnesota, Minneapolis, MN 55455, United States
[b] Department of Chemistry, University of Minnesota, Minneapolis, MN 55455, United States

ARTICLE INFO

Article history:
Received 31 January 2011
Revised 10 March 2011
Available online 17 March 2011

Keywords:
Solid-state NMR
Membrane proteins
Magic angle spinning
Phospholamban
REDOR
Frequency-selective dipolar recoupling
Heteronuclear recoupling

ABSTRACT

We present a new method that combines carbonyl-selective labeling with frequency-selective heteronuclear recoupling to resolve the spectral overlap of magic angle spinning (MAS) NMR spectra of membrane proteins in fluid lipid membranes with broad lines and high redundancy in the primary sequence. We implemented this approach in both heteronuclear ^{15}N–$^{13}C^{\alpha}$ and homonuclear ^{13}C–^{13}C dipolar assisted rotational resonance (DARR) correlation experiments. We demonstrate its efficacy for the membrane protein phospholamban reconstituted in fluid PC/PE/PA lipid bilayers. The main advantage of this method is to discriminate overlapped $^{13}C^{\alpha}$ resonances by strategically labeling the preceding residue. This method is highly complementary to $^{13}C'_{i-1} - {}^{15}N_i - {}^{13}C_i^{\alpha}$ and $^{13}C^{\alpha}_{i-1} - {}^{15}N_{i-1} - {}^{13}C'_i$ experiments to distinguish inter-residue spin systems at a minimal cost to signal-to-noise.

1. Introduction

Magic angle spinning (MAS) and oriented NMR experiments have been widely employed to determine the structure, topology, and dynamics of biomacromolecules [1–3]. These methods are particularly suited for integral membrane proteins, whose association with lipid vesicles limits the use of liquid-state NMR techniques. In the past years, there has been an outburst of MAS methodologies for resonance assignments and distance measurements in membrane protein samples [1,4–13]. Unlike oriented solid-state NMR (SSNMR), which requires a high-degree of orientation with respect to the magnetic field [14–21], MAS sample preparations are more straightforward, making this technique popular in membrane protein structural biology. The strategy to obtain structural parameters for membrane protein structures by MAS is similar to that defined for liquid-state NMR, with the first step involving the tedious and lengthy process of resonance assignments followed by distance and torsion angle measurements. The NMR experiments carried out on micro-crystalline membrane protein samples give highly resolved NMR spectra [22–25], although the lack of a fluid membrane protein environment is a concern, and risks (as with X-ray crystallography) to offer conformational snapshots that may not reflect the physiological conditions of proteins in membranes.

In contrast, the membrane protein samples obtained in fluid lipid membranes [26] display significant line broadening and overlap of resonances, particularly in transmembrane (TM) segments, composed of highly redundant hydrophobic amino acids types (Leu, Ala, Gly, Val, Ile, and Phe) [27]. The helical nature of the majority of membrane proteins, the redundancy of the residue-types, and the line broadening caused by static and dynamic disorder limit the resolution in the ^{15}N and ^{13}C spectra. Only in selected cases do the linewidths enable sequence-specific assignments for non-crystalline uniformly ^{13}C and ^{15}N samples [28–31]. A number of approaches have been proposed to address these challenges: (1) main-chain assignment [32] to identify specific residues based on $^{13}C/^{13}C$ correlation spectra [33], (2) solid-phase peptide synthesis that introduces a minimal number of labeled residues at a time [34–38], and (3) selective [25,39] or reverse biosynthetic labeling [40–43] to achieve *pair-wise* distributions. The second and third methods substantially reduce the number of resonances in the spectrum, making sequential assignments possible. Nevertheless, these labeling approaches used in combination with pulse sequences utilizing several polarization transfer steps have been optimized for protein fibers, crystalline proteins, or lipid-depleted membrane protein samples, and do not perform well for membrane proteins functionally reconstituted in fluid lipid membranes.

An elegant way to resolve complex spectra in a uniformly labeled background is to use rotational echo double resonance

Abbreviations: SSNMR, solid-state NMR; MAS, magic angle spinning; PLN, phospholamban; FDR, frequency-selective dipolar recoupling; DARR, dipolar assisted rotational resonance.

* Corresponding author. Address: 6-155 Jackson Hall, 321 Church St. SE, Minneapolis, MN 55455, United States. Fax: +1 612 625 2163.
E-mail address: vegli001@umn.edu (G. Veglia).

1090-7807/$ - see front matter © 2011 Elsevier Inc. All rights reserved.
doi:10.1016/j.jmr.2011.03.013

(REDOR) difference spectroscopy [44–46]. This experiment is analogous to the spin-echo difference spectroscopy developed for solution NMR [47], which has been applied to deconvolute spectra containing three different isotopically labeled species [48,49]. Similar approaches have been utilized in solid-state NMR to measure short- and long-range distances between nuclei. Since MAS causes *I*–*S* dipolar couplings to average to zero over a complete rotor cycle, 180° recoupling pulses on the *I*-spin applied during the rotor cycle reintroduce the dipolar couplings. By subtracting the spectra obtained with and without recoupling pulses, only *S* resonances that have a measurable dipolar coupling with *I* spins are observed. Significant efforts have been made to achieve frequency-selective REDOR [44] and TEDOR [50] experiments for spectral filtering, heteronuclear magnetization transfer, as well as distance/dihedral angle measurements [7,24,51–60]. One of these methods, the frequency-selective dipolar recoupling (FDR), has been implemented in 1D spectra showing applicability to model amino acid compounds [57,58]. This sequence uses 90° pulses instead of 180° recoupling pulses to *I* spins that makes the average Hamiltonian offset dependent [57].

Here, we combined the FDR approach with carbonyl-selective labeling to obtain unambiguous assignments in $^{15}N/^{13}C^{\alpha}$ and $^{13}C^{\alpha}/^{13}C^{X}$ 2D spectra. This new approach complements the existing experiments for sequential assignment (^{15}N–$^{13}C'$, ^{15}N–$^{13}C^{\alpha}$, $^{13}C^{\alpha}$–^{15}N–$^{13}C'$, $^{13}C'$–^{15}N–$^{13}C^{\alpha}$, etc.) of crowded MAS spectra of membrane proteins. When extended in the third dimension, this approach will increase the spectral resolution for membrane proteins with high primary sequence redundancy, allowing the measurement of inter-residue dipolar correlations.

2. Results

Fig. 1 shows heteronuclear and homonuclear pulse sequences used to correlate ^{15}N–$^{13}C^{\alpha}$ (t_1–t_2) and ^{15}N–$^{13}C^{\alpha}$–$^{13}C^{X}$ (t_1–t_2–t_3) with the FDR block. Following cross-polarization from ^{1}H to ^{15}N, the FDR train of 90° pulses is applied after each rotor cycle (125 μsec) at the $^{13}C'$ frequency (177 ppm). In the middle of rotor cycles, 180° pulses are applied to the ^{15}N channel in order to refocus chemical shift evolution, while allowing for dipolar recoupling to occur between $^{13}C'$ and ^{15}N [57,58]. The pulses utilized XY-4 [62] phasing cycling to ^{15}N (*S* spins) and MLEV-4 [61] to ^{13}C (*I* spins).

In proteins, the covalent $^{13}C'$–^{15}N peptide bond is ~1.3 Å, whereas the two-bond distance is ~2.5 Å, giving maximum dipolar couplings of 1.4 and 0.2 kHz, respectively. The theoretical average Hamiltonian dephasing curves for the two distances are plotted in Fig. 2 using analytical Bessel functions [63]. Note that the dephasing of FDR scales $1/\sqrt{2}$ with respect to the REDOR experiment [58]. From the theoretical curves, it is evident that ^{15}N magnetization with one-bond $^{13}C'$ dipolar couplings is dephased after 1.5–2.0 ms ($\Delta S/S_0 > 0.9$), whereas the magnetization for the two-bond couplings is not dephased ($\Delta S/S_0 < 0.1$). Following the FDR block, ^{15}N chemical shift is evolved during t_1 under ^{1}H TPPM decoupling [64]. The next step uses SPECIFIC-CP [65,66] to transfer magnetization from ^{15}N to $^{13}C^{\alpha}$. Therefore, the FDR selectivity filter combined with the ^{15}N–$^{13}C^{\alpha}$ transfer gives a 2D heteronuclear correlation spectrum of ^{15}N–$^{13}C^{\alpha}$ filtered by the preceding $^{13}C'$ (Fig. 1A). When 90° pulses are applied to $^{13}C'$, the magnetization of the ^{15}N spins covalently attached to $^{13}C'$ will be selectively dephased

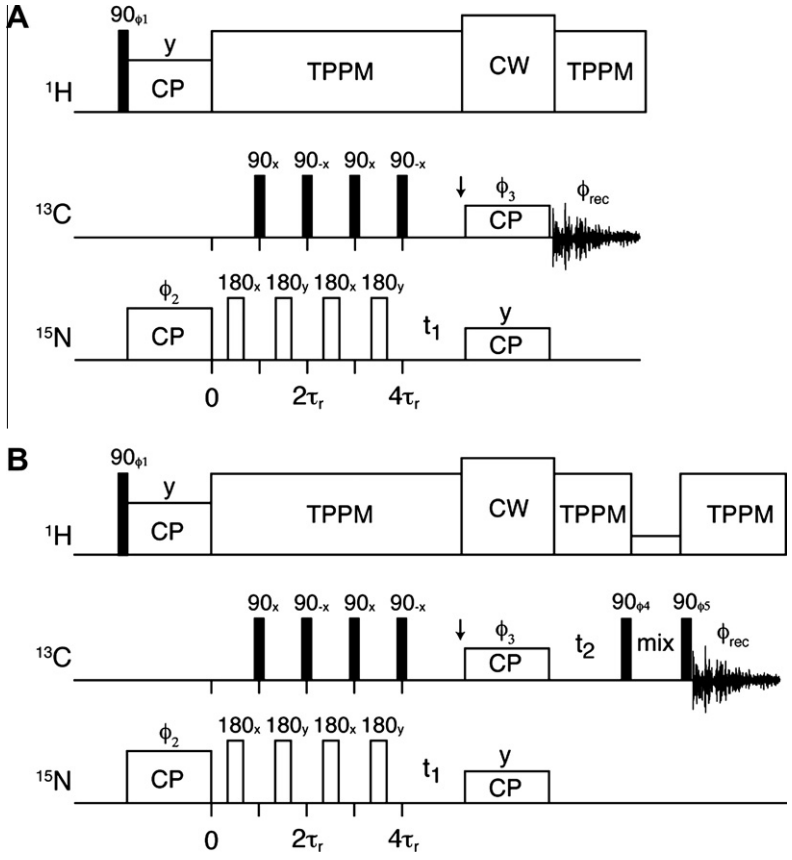

Fig. 1. Pulse sequences used to obtain (A) 2D FDR-^{15}N–$^{13}C^{\alpha}$ and (B) 3D FDR-^{15}N–$^{13}C^{\alpha}$–$^{13}C^{X}$-DARR spectra. The 90° pulses on ^{13}C are phase-cycled with MLEV-4 [61] and applied at the end of each rotor cycle, while the 180° pulses to ^{15}N are applied in the middle of the rotor cycle with XY-4 phase cycling [62]. Phase cycling is as follows: ϕ_1 {x,−x}, ϕ_2 {y}, ϕ_3 {x,x,y,y,−x,−x,−y,−y}, ϕ_4 {y,y,−x,−x,−y,−y,x,x}, ϕ_5 {−y,−y,x,x,y,y,−x,−x}, ϕ_{rec} {x,−x,y,−y,−x,x,−y,y}. Phases ϕ_2 and ϕ_3 are adjusted by 90° to generate phase-sensitive data in t_1 and t_2, respectively.

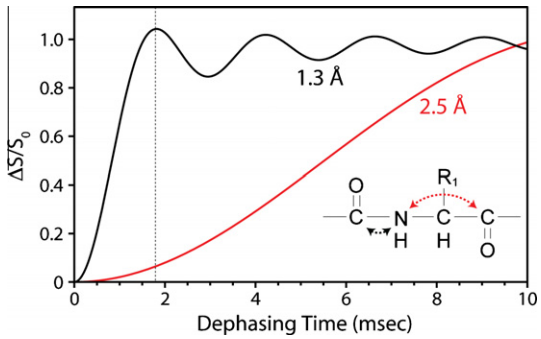

Fig. 2. FDR dephasing $^{15}N\{^{13}C\}$ curves for one-bond (1.3 Å) and two-bond (2.5 Å) $^{13}C'–^{15}N$ distances. The dotted line indicates the maximum dephasing for one-bond transfer, showing less than 0.1 dephasing for the two-bond curve. The FDR dephasing data is scaled by $1/\sqrt{2}$ with respect to the REDOR experiment [44,58].

(filtered-out), while that of the ^{15}N spins attached to $^{12}C'$ will be retained. Subtracting the two experiments results in a spectrum similar to that obtained from the $^{13}C'–^{15}N–^{13}C^{\alpha}$ pulse sequence with double SPECIFIC-CP transfers [28,67,68].

The results from the FDR-$^{15}N–^{13}C^{\alpha}$ 2D spectra on microcrystalline NAVL are shown in Fig. 3. For these experiments, NAVL was labeled [U-^{13}C,^{15}N]-Leu/Val with the acetyl group at natural ^{13}C abundance. The MAS rate was set to 8 kHz and used 2 ms of dipolar dephasing. The experiment with no ^{13}C 90° pulses (reference spectrum) gives two peaks from the two $^{15}N–^{13}C^{\alpha}$ bonds in NAVL (Fig. 3B). In contrast, the experiment with dephasing gives one intense resonance that is 85% of the intensity of the reference spectrum and one that was reduced to 12% intensity (Fig. 3A). The difference spectrum (dephased – reference spectra) gives one intense peak that was assigned to the ^{15}N resonance covalently bonded to $^{13}C'$ (i.e., the Leu peak). These experiments demonstrate the usefulness of the FDR scheme to discriminate between one- and two-bond $^{13}C'–^{15}N$ dipolar couplings in heteronuclear multidimensional correlation experiments.

Filtering one- and two-bond $^{13}C'–^{15}N$ dipolar couplings can also be achieved using the $^{13}C'–^{15}N–^{13}C^{\alpha}$ experiment [28,67,68]. This experiment utilizes two SPECIFIC-CP [65] elements to transfer magnetization from $^{13}C'$ to ^{15}N and then from ^{15}N to $^{13}C^{\alpha}$. To compare the two approaches, we optimized all parameters in each experiment and directly tested the efficiencies with respect to the $^{1}H–^{13}C$ cross-polarization and $^{15}N–^{13}C^{\alpha}$ experiments using NAVL (Fig. 4). The integrated intensities from these spectra are shown in Table 1. We found that the FDR approach gives 36–41% (for 2.0 and 1.5 ms dephasing times) of the signal with respect to the $^{1}H–^{13}C$ cross-polarization experiment for the peak at 61.0 ppm (resonance not dephased), while the largest peak in the $^{13}C'–^{15}N–^{13}C^{\alpha}$ experiment (peak at 56.3 ppm) gives 22% intensity retention. Relative to the $^{15}N–^{13}C^{\alpha}$ spectrum, FDR gives 68–76%, while the $^{13}C'–^{15}N–^{13}C^{\alpha}$ experiment gives 49% efficiency, an improvement in signal-to-noise of 38–55%. Another added benefit of our method is the relative ease of setting up the FDR experiment, which requires calibration of 90° and 180° pulses, while the $^{13}C'–^{15}N–^{13}C^{\alpha}$ experiment requires an additional SPECIFIC-CP transfer, which is sensitive to instrumental instabilities [88].

We also applied the FDR-$^{15}N–^{13}C^{\alpha}$ experiment to the integral membrane protein phospholamban (PLN). The monomeric mutant of PLN (AFA-PLN, C36A/C41F/C46A) was synthesized by solid-phase FMOC chemistry with residues 30–33 labeled [U-^{13}C,^{15}N], resulting in four $^{15}N–^{13}C^{\alpha}$ bonds and three $^{13}C'–^{15}N$ peptide bonds. The protein was reconstituted in 8/1/1 (w/w/w) egg phosphatidylcholine/phosphatidylethanolamine/phosphatidic acid (PC/PE/PA) lipid bilayers at a lipid/protein ratio of 60/1. This ratio is higher than the typical membrane protein samples utilized for MAS spectroscopy and is necessary to maintain the protein structural and functional integrity [69,70]. We acquired 1D (Fig. 5) and 2D spectra (Fig. 6) of the reference and FDR sequence. From these spectra, it is clear that the most upfield peak in the reference spectrum is the only signal that does not change in intensity (Fig. 5A and B, respectively). This is more apparent from the difference spectrum in Fig. 5C, which shows only three peaks. The 2D spectrum is shown in Fig. 6 with a comparison to a standard $^{15}N/^{13}C^{\alpha}$ spectrum obtained with SPECIFIC-CP. It is straightforward to assign the missing peak to Asn^{30}. The incomplete dephasing of the signals in the FDR experiment can result from a small offset of the ^{13}C transmitter from the carbonyl carbons, isotopic dilution in the sample, or protein dynamics that can scale the dipolar couplings.

The 3D version of the FDR-$^{15}N–^{13}C^{\alpha}$-DARR pulse sequence is shown in Fig. 1B. Prior to t_2 evolution, this pulse sequence is identical to the 2D version reported in Fig. 1A. Following SPECIFIC-CP, $^{13}C^{\alpha}$ chemical shifts are evolved during t_2, and then allowed to mix under the dipolar assisted rotational resonance (DARR) condition. This gives a 3D spectrum of $^{15}N–^{13}C^{\alpha}–^{13}C^{X}$ ($t_1–t_2–t_3$). *The advantage of this method is to discriminate overlapped C^{α} resonances by strategically labeling the preceding residue (e.g., $^{13}C'$).* The 2D spectra without evolution of ^{15}N is shown in Fig. 7, and demonstrates that the FDR pulse element filters out more than 80% of the signals from the reference spectrum.

3. Discussion

Sequence-specific assignments in MAS spectra of membrane proteins in fluid lipid membranes are a challenging endeavor. Several SSNMR studies on membrane proteins have reported residue-specific assignments that fail to give the atomic resolution provided for in crystalline or synthetically labeled samples. To

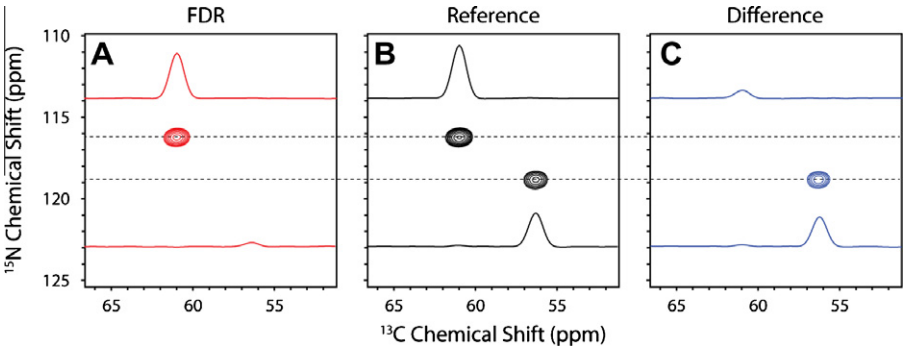

Fig. 3. FDR-$^{15}N–^{13}C^{\alpha}$ spectra for NAVL. Spectra were acquired with (FDR, panel A) and without ^{13}C 90° pulses (reference, panel B). A total dephasing time of 2 ms was used with an MAS rate of 8 kHz. (C) Subtraction of the FDR spectrum from that of the reference. Note that in the subtracted spectrum, the noise increases by a factor of $\sqrt{2}$.

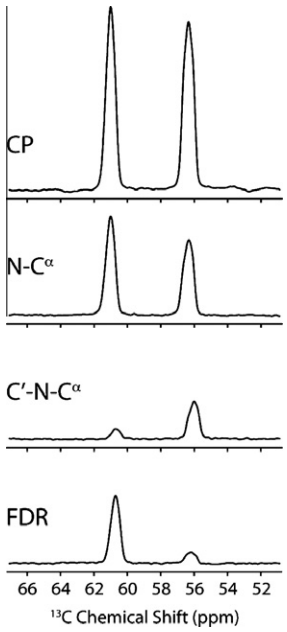

Fig. 4. Comparison of ^{1}H–^{13}C cross-polarization, ^{15}N–$^{13}C^{\alpha}$ SPECIFIC-CP, $^{13}C'$–^{15}N–$^{13}C^{\alpha}$ double SPECIFIC-CP, and FDR-^{15}N–$^{13}C^{\alpha}$ (2.0 ms dephasing time) experiments. The integrated intensities from these spectra are shown in Table 1.

Table 1
Transfer efficiencies calculated from integrated 1D NAVL spectra for the ^{15}N–$^{13}C^{\alpha}$, $^{13}C'$–^{15}N–$^{13}C^{\alpha}$, and FDR–^{15}N–$^{13}C^{\alpha}$ experiments in Fig. 4 expressed as a percentage from that of the cross-polarization (^{1}H–^{13}C) experiment. Data are normalized with respect to each peak in NAVL. The FDR experiment was conducted using total dephasing times of 1.5 and 2.0 ms. Errors for all values are less than 0.1%.

Experiment	Peak 1 (C^{α} = 61.0 ppm) (%)	Peak 2 (C^{α} = 56.3 ppm) (%)
Cross-polarization	100	100
N–C^{α}	53.3	44.5
C′–N–C^{α}	5.6	22.0
FDR–N–C^{α} (1.5 ms)	40.7	9.6
FDR–N–C^{α} (2.0 ms)	36.3	6.3

address these problems, we propose an approach that is based on carbonyl-selective labeling combined with frequency-selective dipolar recoupling experiments and SPECIFIC-CP. These experiments will be useful to obtain specific assignments, while retaining better signal to noise (~68–76%) with respect to a 2D ^{15}N–$^{13}C^{\alpha}$ experiment using SPECIFIC-CP than the $^{13}C'$–^{15}N–$^{13}C^{\alpha}$ experiment (~49%).

Selective labeling strategies have become useful to reduce the complexity of spectra and the assignment process in general. A common procedure is to grow bacteria and overexpress target proteins in unlabeled growth media enriched with one or more ^{13}C and ^{15}N amino acids [71]. Alternatively, one can use reverse labeling [40], where unlabeled amino acids are added to the isotopically enriched growth media. Both give a significant reduction in spectral complexity. More advanced strategies involve the use of labeled metabolic precursors (reviewed in [71]). This approach has been primarily used for reducing the number of ^{13}C–^{13}C scalar couplings [41,43,72], while maintaining a significant amount of ^{15}N and ^{13}C labels in the protein. The most robust protocols have been developed for labeling $^{13}C'$, $^{13}C^{\alpha}$, and $^{13}C^{\beta}$ with the goal of performing ^{13}C solution NMR relaxation studies without the interference of covalently attached ^{13}C nuclei [72,73]. In particular, $^{13}C'$ labels can be incorporated in several different residues without the need to reduce the labeling of the $^{13}C^{\alpha}$ (reverse labeling + labeled amino acids). The ideal use of our approach from a sensitivity perspective is to label all $^{13}C^{\alpha}$ in the protein and incorporate $^{13}C'$ labels in several different residue types. This can be accomplished using 2-^{13}C-glucose [73] and supplementing the growth medium with [U-^{13}C] labeled leucine. This application would allow i + 1 residues with respect to leucine to be filtered out in the FDR-NC$^{\alpha}$ experiment, and clearly identified in the difference spectrum, which would simplify the assignment. Further advancements will be to combine carbonyl-selective labeling with combinatorial approaches used to assign overlapped spectra in solution NMR [74–79]. In particular, one can apply the FDR approach to $^{13}C^{\alpha}$ and $^{13}C^{\beta}$ atoms to achieve frequency selective filters for assignment, or can use any of the labeling strategies discussed above to achieve pair-wise $^{13}C'$–^{15}N labels to simplify the spectrum.

4. Conclusions

The approach presented here is a sensitive complement to the sequential $^{13}C'$–^{15}N–$^{13}C^{\alpha}$ experiments [28,67,68]. In particular, our method gives 38–55% more signal than the $^{13}C'$–^{15}N–$^{13}C^{\alpha}$ experiment. It allows one to select $^{12}C'$–^{15}N–$^{13}C^{\alpha}$ patterns while filtering out the $^{13}C'$–^{15}N–$^{13}C^{\alpha}$ patterns, with a sensitivity of ~68–76% relative to the standard ^{15}N–$^{13}C^{\alpha}$ spectrum obtained with SPECIFIC-CP. In addition, our method allows for the possibility of identifying chemically identical proteins with differential labeling in a single sample. Frequency selective methods combined with novel isotope incorporation such as the method described in this paper and others [1,41,68,80–83] will be useful to making sequence-specific assignments in fluid membrane protein samples and other samples with non-crystalline linewidths.

5. Experimental

5.1. Sample preparation

N-acetyl-valyl-leucine was synthesized using solid-phase synthesis from FMOC-[U-^{13}C,^{15}N]-Leu and FMOC-[U-^{13}C,^{15}N]-Val (Sigma–Aldrich, Isotec). The N-terminus of valine was acetylated

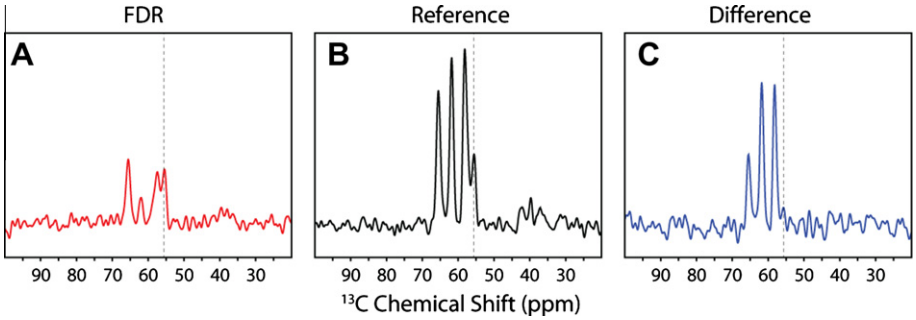

Fig. 5. FDR-^{15}N–$^{13}C^{\alpha}$ spectra for AFA-PLN labeled [U-^{13}C,^{15}N] at residues 30–33. 1D spectra were acquired with (FDR, panel A) and without ^{13}C 90° pulses (reference, panel B). A total dephasing time of 2 ms was used with an MAS rate of 8 kHz. (C) Subtraction of the FDR spectrum from the reference.

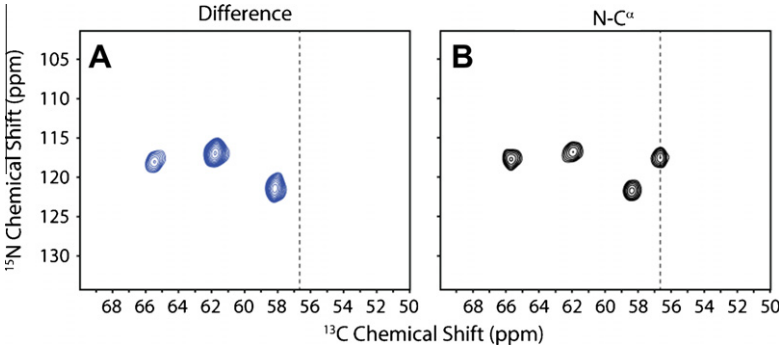

Fig. 6. 2D FDR-^{15}N–^{13}C$^{\alpha}$ spectra for AFA-PLN labeled [U-^{13}C,^{15}N] at residues 30–33. (A) Difference spectrum for AFA-PLN$^{30-33}$ using similar parameters as that in Fig. 5. (B) ^{15}N–^{13}C$^{\alpha}$ spectrum of AFA-PLN$^{30-33}$.

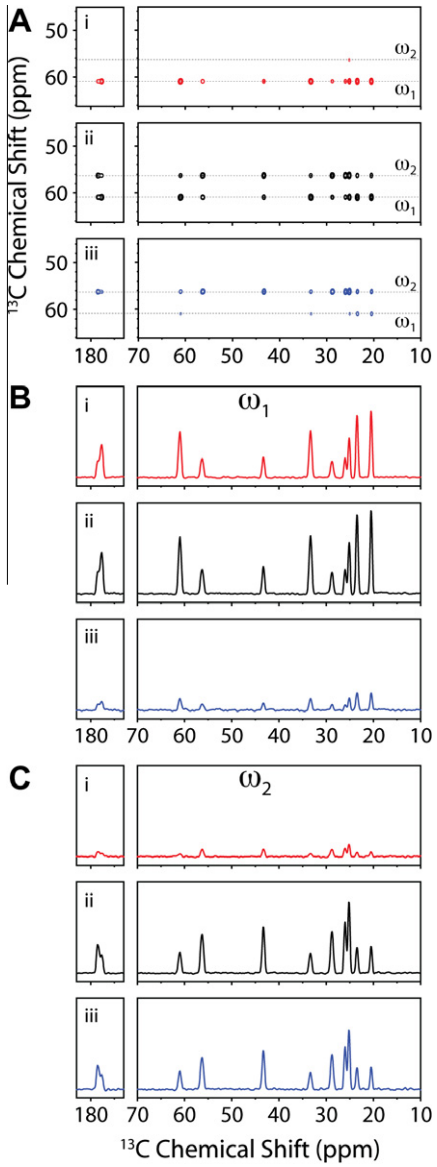

Fig. 7. FDR-^{13}C$^{\alpha}$–^{13}C^{X}-DARR spectra for NAVL. (A) Spectra were acquired with (FDR, panel i) and without ^{13}C 90° pulses (reference, panel ii) using the pulse sequence in Fig. 1B. A total dephasing time of 2 ms was used with an MAS rate of 8 kHz. (iii) Subtraction of the FDR spectrum from that of the reference. A 100 ms DARR mixing time was used. Panels B and C show the 1D traces from the 2D spectra in panel A.

by acetic anhydride at natural ^{13}C abundance. AFA-PLN was labeled at residues 30–33 with 99% [U-^{13}C,^{15}N]-Asn, Leu, Phe, and Ile (Sigma–Aldrich, Isotec) using solid-phase synthesis as described previously [16]. Labeling was checked by solution NMR in dodecylphosphocholine micelles [70] and mass-spectrometry. PLN (~2 mg) was solubilized in 500 µl trifluoroethanol and added to 15 mg egg PC/PE/PA lipids (8/1/1, w/w/w; Avanti Polar Lipids, Albaster, AL) in chloroform. The solvent was dried under a stream of nitrogen gas and placed in a vacuum dessicator overnight to remove residual organics. Vesicles were prepared by adding 2 ml buffer (20 mM HEPES pH 7.0, 100 mM potassium chloride, 10 mM dithiothreitol, and 3 mM sodium azide) to the lipid/protein and flash frozen 3–4 times in liquid nitrogen. Samples were then spun for 30 min at 200,000*g* in a benchtop ultracentrifuge. The pellet was transferred to a 3.2 mm thin-walled rotor with sample spacers (Agilent, Fort Collins, CO) to avoid dehydration.

5.2. Solid-state NMR spectroscopy

NMR experiments were performed using a VNMRS spectrometer operating at a ^{1}H frequency of 600 MHz, with a 3.2 mm bioMAS probe [84], an MAS spinning rate of 8 kHz (υ_R), and a temperature of 20 °C. All experiments utilized cross-polarization from ^{1}H (61 kHz) to ^{15}N (45 kHz) satisfying the $n = 2$ condition for 1.0 ms (PLN) or 2.0 ms (NAVL). The FDR sequence used 5.5 µsec 90° pulses (45.5 kHz) applied to ^{13}C′ and 11 µsec 180° pulses (45.5 kHz) centered on the ^{15}N resonances. The ^{13}C pulses were phase-cycled using MLEV-4 [61], while those to ^{15}N were cycled using XY-4 [62]. A total of 12 (1.5 ms) or 16 (2.0 ms) rotor periods were employed to achieve dipolar dephasing from ^{13}C′. The ^{15}N dimension had a spectral width of 2 kHz and was evolved for 12 and 50 increments for PLN and NAVL experiments, respectively. Transfers from ^{15}N to ^{13}C$^{\alpha}$ were achieved by moving the ^{13}C carrier frequency to ^{13}C$^{\alpha}$ (59.2 ppm) and performing SPECIFIC-CP [65], which is related to the double cross-polarization experiment [66]. Spin-lock was applied to ^{15}N at $\frac{5}{2}\frac{\omega_R}{2\pi}$ (20 kHz) and ^{13}C$^{\alpha}$ at $\frac{3}{2}\frac{\omega_R}{2\pi}$ (12 kHz) or ^{13}C′ at $\frac{7}{2}\frac{\omega_R}{2\pi}$ (28 kHz). The SPECIFIC-CP time was 5–6 ms utilizing either a linear (±10% γB_1) or adiabatic ramp ($\frac{\Delta}{2\pi}$ = ~2 kHz, $\frac{\beta}{2\pi}$ = ~0.6 kHz) [89] to ^{13}C$^{\alpha}$ or ^{13}C′ for reducing the sensitivity to instrumental instability [88]. The adiabatic ramp was used only to acquire spectra in Fig. 4 in order to achieve the optimal transfers for the ^{13}C′–^{15}N–^{13}C$^{\alpha}$ experiment (two SPECIFIC-CP transfers). The direct ^{13}C spectral width was 100 kHz and was acquired for 20 ms under TPPM [64] ^{1}H decoupling at 100 kHz. For the NAVL 2D experiments, eight scans were collected with a recycle delay of 4 s. The ^{13}C–^{13}C FDR experiment used an indirect ^{13}C spectral width of 16 kHz, 50 increments, and a DARR [85] mixing time of 100 ms set to $n = 1$ rotary resonance condition. The 2D FDR-^{15}N–^{13}C$^{\alpha}$ PLN experiment used 2048 scans with a recycle delay of 2 s. The 1D FDR experiment used 20,000 scans with a recycle delay of 2 s. The CH_2 resonance of adamantane was referenced to 40.48 ppm [86] and indirectly to ^{15}N using the relative frequency ratio between ^{15}N and ^{13}C of Ξ = 0.402979946 [87].

Acknowledgments

We thank Dan Mullen for synthesizing NAVL and PLN and T. Gopinath, Raffaello Verardi, and Martin Gustavsson for helpful discussions. This work was supported by the National Institute of Health (GM64742 to G.V.).

References

[1] M. Baldus, Correlation experiments for assignment and structure elucidation of immobilized polypeptides under magic angle spinning, Prog. Nucl. Magn. Reson. Spectrosc. 41 (2002) 1–47.
[2] S.J. Opella, C. Ma, F.M. Marassi, Nuclear magnetic resonance of membrane-associated peptides and proteins, Methods Enzymol. 339 (2001) 285–313.
[3] A. Watts, A.S. Ulrich, D.A. Middleton, Membrane protein structure: the contribution and potential of novel solid state NMR approaches, Mol. Membr. Biol. 12 (1995) 233–246.
[4] A.B. Nielsen, L.A. Straaso, A.J. Nieuwkoop, C.M. Rienstra, M. Bjerring, N.C. Nielsen, Broadband heteronuclear solid-state NMR experiments by exponentially modulated dipolar recoupling without decoupling, J. Phys. Chem. Lett. 1 (2010) 1952–1956.
[5] J.R. Lewandowski, G. De Paepe, R.G. Griffin, Proton assisted insensitive nuclei cross polarization, J. Am. Chem. Soc. 129 (2007) 728–729.
[6] C.P. Jaroniec, C. Filip, R.G. Griffin, 3D TEDOR NMR experiments for the simultaneous measurement of multiple carbon–nitrogen distances in uniformly (13)C, (15)N-labeled solids, J. Am. Chem. Soc. 124 (2002) 10728–10742.
[7] N.A. Oyler, R. Tycko, Conformational constraints in solid-state NMR of uniformly labeled polypeptides from double single-quantum-filtered rotational echo double resonance, Magn. Reson. Chem. 45 (Suppl. 1) (2007) S101–S106.
[8] M.J. Bayro, M. Huber, R. Ramachandran, T.C. Davenport, B.H. Meier, M. Ernst, R.G. Griffin, Dipolar truncation in magic-angle spinning NMR recoupling experiments, J. Chem. Phys. 130 (2009) 114506.
[9] R. Verel, B.H. Meier, Polarization-transfer methods in solid-state magic-angle-spinning NMR: adiabatic CN pulse sequences, ChemPhysChem 5 (2004) 851–862.
[10] I. Bertini, L. Emsley, M. Lelli, C. Luchinat, J. Mao, G. Pintacuda, Ultrafast MAS solid-state NMR permits extensive ^{13}C and ^{1}H detection in paramagnetic metalloproteins, J. Am. Chem. Soc. 132 (2010) 5558–5559.
[11] W.T. Franks, B.J. Wylie, H.L. Schmidt, A.J. Nieuwkoop, R.M. Mayrhofer, G.J. Shah, D.T. Graesser, C.M. Rienstra, Dipole tensor-based atomic-resolution structure determination of a nanocrystalline protein by solid-state NMR, Proc. Natl. Acad. Sci. USA 105 (2008) 4621–4626.
[12] D.H. Zhou, K.D. Kloepper, K.A. Winter, C.M. Rienstra, Band-selective ^{13}C homonuclear 3D spectroscopy for solid proteins at high field with rotor-synchronized soft pulses, J. Biomol. NMR 34 (2006) 245–257.
[13] P.S. Nadaud, J.J. Helmus, N. Hofer, C.P. Jaroniec, Long-range structural restraints in spin-labeled proteins probed by solid-state nuclear magnetic resonance spectroscopy, J. Am. Chem. Soc. 129 (2007) 7502–7503.
[14] A.A. De Angelis, A.A. Nevzorov, S.H. Park, S.C. Howell, A.A. Mrse, S.J. Opella, High-resolution NMR spectroscopy of membrane proteins in aligned bicelles, J. Am. Chem. Soc. 126 (2004) 15340–15341.
[15] U.H. Durr, K. Yamamoto, S.C. Im, L. Waskell, A. Ramamoorthy, Solid-state NMR reveals structural and dynamical properties of a membrane-anchored electron-carrier protein, cytochrome b5, J. Am. Chem. Soc. 129 (2007) 6670–6671.
[16] N.J. Traaseth, L. Shi, R. Verardi, D. Mullen, G. Barany, G. Veglia, Determination of membrane protein structure and topology using a hybrid solution and solid-state NMR approach, Proc. Natl. Acad. Sci. USA 106 (2009) 10165–10170.
[17] J. Hu, T. Asbury, S. Achuthan, C. Li, R. Bertram, J.R. Quine, R. Fu, T.A. Cross, Backbone structure of the amantadine-blocked trans-membrane domain M2 proton channel from Influenza A virus, Biophys. J. 92 (2007) 4335–4343.
[18] C. Aisenbrey, B. Bechinger, Investigations of polypeptide rotational diffusion in aligned membranes by 2H and ^{15}N solid-state NMR spectroscopy, J. Am. Chem. Soc. 126 (2004) 16676–16683.
[19] A. Naito, Structure elucidation of membrane-associated peptides and proteins in oriented bilayers by solid-state NMR spectroscopy, Solid State Nucl. Magn. Reson. 36 (2009) 67–76.
[20] T. Vosegaard, M. Kamihira-Ishijima, A. Watts, N.C. Nielsen, Helix conformations in 7TM membrane proteins determined using oriented-sample solid-state NMR with multiple residue-specific ^{15}N labeling, Biophys. J. 94 (2008) 241–250.
[21] R. Fu, E.D. Gordon, D.J. Hibbard, M. Cotten, High resolution heteronuclear correlation NMR spectroscopy of an antimicrobial peptide in aligned lipid bilayers: peptide–water interactions at the water-bilayer interface, J. Am. Chem. Soc. 131 (2009) 10830–10831.
[22] Y. Li, D.A. Berthold, R.B. Gennis, C.M. Rienstra, Chemical shift assignment of the transmembrane helices of DsbB, a 20-kDa integral membrane enzyme, by 3D magic-angle spinning NMR spectroscopy, Protein Sci. 17 (2008) 199–204.
[23] L. Huang, A.E. McDermott, Partial site-specific assignment of a uniformly (13)C, (15)N enriched membrane protein, light-harvesting complex 1 (LH1), by solid state NMR, Biochim. Biophys. Acta 1777 (2008) 1098–1108.
[24] J. Yang, M.L. Tasayco, T. Polenova, Magic angle spinning NMR experiments for structural studies of differentially enriched protein interfaces and protein assemblies, J. Am. Chem. Soc. 130 (2008) 5798–5807.
[25] Y. Han, J. Ahn, J. Concel, I.J. Byeon, A.M. Gronenborn, J. Yang, T. Polenova, Solid-state NMR studies of HIV-1 capsid protein assemblies, J. Am. Chem. Soc. 132 (2010) 1976–1987.
[26] O.C. Andronesi, S. Becker, K. Seidel, H. Heise, H.S. Young, M. Baldus, Determination of membrane protein structure and dynamics by magic-angle-spinning solid-state NMR spectroscopy, J. Am. Chem. Soc. 127 (2005) 12965–12974.
[27] M.B. Ulmschneider, M.S. Sansom, Amino acid distributions in integral membrane protein structures, Biochim. Biophys. Acta 1512 (2001) 1–14.
[28] L. Shi, M.A. Ahmed, W. Zhang, G. Whited, L.S. Brown, V. Ladizhansky, Three-dimensional solid-state NMR study of a seven-helical integral membrane proton pump – structural insights, J. Mol. Biol. 386 (2009) 1078–1093.
[29] M. Etzkorn, S. Martell, O.C. Andronesi, K. Seidel, M. Engelhard, M. Baldus, Secondary structure, dynamics, and topology of a seven-helix receptor in native membranes, studied by solid-state NMR spectroscopy, Angew. Chem. Int. Ed. Engl. 46 (2007) 459–462.
[30] C. Ader, R. Schneider, S. Hornig, P. Velisetty, E.M. Wilson, A. Lange, K. Giller, I. Ohmert, M.F. Martin-Eauclaire, D. Trauner, S. Becker, O. Pongs, M. Baldus, A structural link between inactivation and block of a K+ channel, Nat. Struct. Mol. Biol. 15 (2008) 605–612.
[31] M.P. Bhate, B.J. Wylie, L. Tian, A.E. McDermott, Conformational dynamics in the selectivity filter of KcsA in response to potassium ion concentration, J. Mol. Biol. 401 (2010) 155–166.
[32] S.W. Englander, A.J. Wand, Main-chain-directed strategy for the assignment of ^{1}H NMR spectra of proteins, Biochemistry 26 (1987) 5953–5958.
[33] K. Seidel, O.C. Andronesi, J. Krebs, C. Griesinger, H.S. Young, S. Becker, M. Baldus, Structural characterization of Ca(2+)-ATPase-bound phospholamban in lipid bilayers by solid-state nuclear magnetic resonance (NMR) spectroscopy, Biochemistry 47 (2008) 4369–4376.
[34] C.P. Jaroniec, C.E. MacPhee, V.S. Bajaj, M.T. McMahon, C.M. Dobson, R.G. Griffin, High-resolution molecular structure of a peptide in an amyloid fibril determined by magic angle spinning NMR spectroscopy, Proc. Natl. Acad. Sci. USA 101 (2004) 711–716.
[35] A.T. Petkova, Y. Ishii, J.J. Balbach, O.N. Antzutkin, R.D. Leapman, F. Delaglio, R. Tycko, A structural model for Alzheimer's beta-amyloid fibrils based on experimental constraints from solid state NMR, Proc. Natl. Acad. Sci. USA 99 (2002) 16742–16747.
[36] S.O. Smith, T. Kawakami, W. Liu, M. Ziliox, S. Aimoto, Helical structure of phospholamban in membrane bilayers, J. Mol. Biol. 313 (2001) 1139–1148.
[37] E. Hughes, D.A. Middleton, Solid-state NMR reveals structural changes in phospholamban accompanying the functional regulation of Ca^{2+}ATPase, J. Biol. Chem. 278 (2003) 20835–20842.
[38] S.D. Cady, K. Schmidt-Rohr, J. Wang, C.S. Soto, W.F. Degrado, M. Hong, Structure of the amantadine binding site of influenza M2 proton channels in lipid bilayers, Nature 463 (2010) 689–692.
[39] S. Ahuja, V. Hornak, E.C. Yan, N. Syrett, J.A. Goncalves, A. Hirshfeld, M. Ziliox, T.P. Sakmar, M. Sheves, P.J. Reeves, S.O. Smith, M. Eilers, Helix movement is coupled to displacement of the second extracellular loop in rhodopsin activation, Nat. Struct. Mol. Biol. 16 (2009) 168–175.
[40] G.W. Vuister, S.-. Kim, C. Wu, A. Bax, 2D and 3D NMR study of phenylalanine residues in proteins by reverse isotopic labeling, J. Am. Chem. Soc. 116 (1994) 9206–9210.
[41] M. Hong, K. Jakes, Selective and extensive ^{13}C labeling of a membrane protein for solid-state NMR investigations, J. Biomol. NMR 14 (1999) 71–74.
[42] H. Heise, W. Hoyer, S. Becker, O.C. Andronesi, D. Riedel, M. Baldus, Molecular-level secondary structure, polymorphism, and dynamics of full-length alpha-synuclein fibrils studied by solid-state NMR, Proc. Natl. Acad. Sci. USA 102 (2005) 15871–15876.
[43] F. Castellani, B. van Rossum, A. Diehl, M. Schubert, K. Rehbein, H. Oschkinat, Structure of a protein determined by solid-state magic-angle-spinning NMR spectroscopy, Nature 420 (2002) 98–102.
[44] T. Gullion, J. Schaefer, Rotational-echo double-resonance NMR, J. Magn. Reson. 81 (1989) 196–200.
[45] J. Yang, P.D. Parkanzky, M.L. Bodner, C.A. Duskin, D.P. Weliky, Application of REDOR subtraction for filtered MAS observation of labeled backbone carbons of membrane-bound fusion peptides, J. Magn. Reson. 159 (2002) 101–110.
[46] S. Matsuoka, J. Schaefer, Double-quantum filtered rotational-echo double resonance, J. Magn. Reson. 183 (2006) 252–258.
[47] G.W. Vuister, A.C. Wang, A. Bax, Measurement of three-bond nitrogen–carbon J couplings in proteins uniformly enriched in ^{15}N and ^{13}C, J. Am. Chem. Soc. 115 (1993) 5334–5335.
[48] L.R. Masterson, M. Tonelli, J.L. Markley, G. Veglia, Simultaneous detection and deconvolution of congested NMR spectra containing three isotopically labeled species, J. Am. Chem. Soc. 130 (2008) 7818–7819.
[49] M. Tonelli, L.R. Masterson, K. Hallenga, G. Veglia, J.L. Markley, Carbonyl carbon label selective (CCLS) ^{1}H–^{15}N HSQC experiment for improved detection of backbone ^{13}C–^{15}N cross peaks in larger proteins, J. Biomol. NMR 39 (2007) 177–185.
[50] A.W. Hing, S. Vega, J. Schaefer, Transferred-echo double-resonance NMR, J. Magn. Reson. 96 (1992) 205–209.

[51] C.P. Jaroniec, B.A. Tounge, J. Herzfeld, R.G. Griffin, Frequency selective heteronuclear dipolar recoupling in rotating solids: accurate (13)C–(15)N distance measurements in uniformly (13)C, (15)N-labeled peptides, J. Am. Chem. Soc. 123 (2001) 3507–3519.
[52] S. Li, Y. Su, W. Luo, M. Hong, Water–protein interactions of an arginine-rich membrane peptide in lipid bilayers investigated by solid-state nuclear magnetic resonance spectroscopy, J. Phys. Chem. B 114 (2010) 4063–4069.
[53] M. Hong, R.G. Griffin, Resonance assignments for solid peptides by dipolar-mediated $^{13}C/^{15}N$ correlation solid-state NMR, J. Am. Chem. Soc. 120 (1998) 7113–7114.
[54] V. Chevelkov, K. Faelber, A. Diehl, U. Heinemann, H. Oschkinat, B. Reif, Detection of dynamic water molecules in a microcrystalline sample of the SH3 domain of alpha-spectrin by MAS solid-state NMR, J. Biomol. NMR 31 (2005) 295–310.
[55] L. Kaustov, S. Kababya, V. Belakhov, T. Baasov, Y. Shoham, A. Schmidt, Inhibition mode of a bisubstrate inhibitor of KDO8P synthase: a frequency-selective REDOR solid-state and solution NMR characterization, J. Am. Chem. Soc. 125 (2003) 4662–4669.
[56] C.A. Klug, W.L. Zhu, K. Tasaki, J. Schaefer, Orientational order of locally parallel chain segments in glassy polycarbonate from C-13–C-13 dipolar couplings, Macromolecules 30 (1997) 1734–1740.
[57] A.E. Bennett, C.M. Rienstra, P.T. Lansbury, R.G. Griffin, Frequency-selective heteronuclear dephasing by dipole couplings in spinning and static solids, J. Chem. Phys. 105 (1996) 10289–10299.
[58] A.E. Bennett, L.R. Becerra, R.G. Griffin, Frequency-selective heteronuclear recoupling in rotating solids, J. Chem. Phys. 100 (1994) 812–814.
[59] I. Schnell, B. Langer, S.H. Sontjens, M.H. van Genderen, R.P. Sijbesma, H.W. Spiess, Inverse detection and heteronuclear editing in $^{1}H–^{15}N$ correlation and $^{1}H–^{1}H$ double-quantum NMR spectroscopy in the solid state under fast MAS, J. Magn. Reson. 150 (2001) 57–70.
[60] X.L. Yao, K. Schmidt-Rohr, M. Hong, Medium- and long-distance $^{1}H–^{13}C$ heteronuclear correlation NMR in solids, J. Magn. Reson. 149 (2001) 139–143.
[61] M. Levitt, R. Freeman, T. Frenkel, Broadband heteronuclear decoupling, J. Magn. Reson. 47 (1982) 328–330.
[62] T. Gullion, D.B. Baker, M.S. Conradi, New, compensated Carr-Purcell sequences, J. Magn. Reson. 89 (1990) 479–484.
[63] K.T. Mueller, Analytic solutions for the time evolution of dipolar-dephasing NMR signals, J. Magn. Reson. A 113 (1995) 81–93.
[64] A.E. Bennett, C.M. Rienstra, M. Auger, K.V. Lakshmi, R.G. Griffin, Heteronuclear decoupling in rotating solids, J. Chem. Phys. 103 (1995) 6951–6958.
[65] M. Baldus, A.T. Petkova, J.H. Herzfeld, R.G. Griffin, Cross polarization in the tilted frame: assignment and spectral simplification in heteronuclear spin systems, Mol. Phys. 95 (1998) 1197–1207.
[66] J. Schaefer, R.A. McKay, E.O. Stejskal, Double-cross-polarization NMR of solids, J. Magn. Reson. 34 (1979) 443–447.
[67] Y. Li, D.A. Berthold, H.L. Frericks, R.B. Gennis, C.M. Rienstra, Partial (13)C and (15)N chemical-shift assignments of the disulfide-bond-forming enzyme DsbB by 3D magic-angle spinning NMR spectroscopy, ChemBioChem 8 (2007) 434–442.
[68] A. Schuetz, C. Wasmer, B. Habenstein, R. Verel, J. Greenwald, R. Riek, A. Bockmann, B.H. Meier, Protocols for the sequential solid-state NMR spectroscopic assignment of a uniformly labeled 25 kDa protein: HET-s(1-227), ChemBioChem 11 (2010) 1543–1551.
[69] N.J. Traaseth, J.J. Buffy, J. Zamoon, G. Veglia, Structural dynamics and topology of phospholamban in oriented lipid bilayers using multidimensional solid-state NMR, Biochemistry 45 (2006) 13827–13834.
[70] N.J. Traaseth, K.N. Ha, R. Verardi, L. Shi, J.J. Buffy, L.R. Masterson, G. Veglia, Structural and dynamic basis of phospholamban and sarcolipin inhibition of Ca(2+)-ATPase, Biochemistry 47 (2008) 3–13.
[71] L.Y. Lian, D.A. Middleton, Labelling approaches for protein structural studies by solution-state and solid-state NMR, Prog. Nucl. Magn. Reson. Spectrosc. 39 (2001) 171–190.
[72] D.M. LeMaster, D.M. Kushlan, Dynamical mapping of *E. coli* thioredoxin via C-13 NMR relaxation analysis, J. Am. Chem. Soc. 118 (1996) 9255–9264.
[73] P. Lundstrom, K. Teilum, T. Carstensen, I. Bezsonova, S. Wiesner, D.F. Hansen, T.L. Religa, M. Akke, L.E. Kay, Fractional ^{13}C enrichment of isolated carbons using [1-^{13}C]- or [2-^{13}C]-glucose facilitates the accurate measurement of dynamics at backbone Calpha and side-chain methyl positions in proteins, J. Biomol. NMR 38 (2007) 199–212.
[74] J. Shi, J.G. Pelton, H.S. Cho, D.E. Wemmer, Protein signal assignments using specific labeling and cell-free synthesis, J. Biomol. NMR 28 (2004) 235–247.
[75] P.S. Wu, K. Ozawa, S. Jergic, X.C. Su, N.E. Dixon, G. Otting, Amino-acid type identification in ^{15}N-HSQC spectra by combinatorial selective ^{15}N-labelling, J. Biomol. NMR 34 (2006) 13–21.
[76] J. Weigelt, M. van Dongen, J. Uppenberg, J. Schultz, M. Wikstrom, Site-selective screening by NMR spectroscopy with labeled amino acid pairs, J. Am. Chem. Soc. 124 (2002) 2446–2447.
[77] N. Trbovic, C. Klammt, A. Koglin, F. Lohr, F. Bernhard, V. Dotsch, Efficient strategy for the rapid backbone assignment of membrane proteins, J. Am. Chem. Soc. 127 (2005) 13504–13505.
[78] M.J. Sweredoski, K.J. Donovan, B.D. Nguyen, A.J. Shaka, P. Baldi, Minimizing the overlap problem in protein NMR: a computational framework for precision amino acid labeling, Bioinformatics 23 (2007) 2829–2835.
[79] S. Reckel, S. Sobhanifar, B. Schneider, F. Junge, D. Schwarz, F. Durst, F. Lohr, P. Guntert, F. Bernhard, V. Dotsch, Transmembrane segment enhanced labeling as a tool for the backbone assignment of alpha-helical membrane proteins, Proc. Natl. Acad. Sci. USA 105 (2008) 8262–8267.
[80] L.J. Sperling, D.A. Berthold, T.L. Sasser, V. Jeisy-Scott, C.M. Rienstra, Assignment strategies for large proteins by magic-angle spinning NMR: the 21-kDa disulfide-bond-forming enzyme DsbA, J. Mol. Biol. 399 (2010) 268–282.
[81] V.A. Higman, J. Flinders, M. Hiller, S. Jehle, S. Markovic, S. Fiedler, B.J. van Rossum, H. Oschkinat, Assigning large proteins in the solid state: a MAS NMR resonance assignment strategy using selectively and extensively ^{13}C-labelled proteins, J. Biomol. NMR 44 (2009) 245–260.
[82] S. Jehle, K. Rehbein, A. Diehl, B.J. van Rossum, Amino-acid selective experiments on uniformly ^{13}C and ^{15}N labeled proteins by MAS NMR: filtering of lysines and arginines, J. Magn. Reson. 183 (2006) 324–328.
[83] M.L. Bodner, C.M. Gabrys, P.D. Parkanzky, J. Yang, C.A. Duskin, D.P. Weliky, Temperature dependence and resonance assignment of ^{13}C NMR spectra of selectively and uniformly labeled fusion peptides associated with membranes, Magn. Reson. Chem. 42 (2004) 187–194.
[84] J.A. Stringer, C.E. Bronnimann, C.G. Mullen, D.H. Zhou, S.A. Stellfox, Y. Li, E.H. Williams, C.M. Rienstra, Reduction of RF-induced sample heating with a scroll coil resonator structure for solid-state NMR probes, J. Magn. Reson. 173 (2005) 40–48.
[85] K. Takegoshi, S. Nakamura, T. Terao, $^{13}C–^{1}H$ dipolar-assisted rotational resonance in magic-angle spinning NMR, Chem. Phys. Lett. 344 (2001) 631–637.
[86] C.R. Morcombe, K.W. Zilm, Chemical shift referencing in MAS solid state NMR, J. Magn. Reson. 162 (2003) 479–486.
[87] D.S. Wishart, C.G. Bigam, J. Yao, F. Abildgaard, H.J. Dyson, E. Oldfield, J.L. Markley, B.D. Sykes, ^{1}H, ^{13}C and ^{15}N chemical shift referencing in biomolecular NMR, J. Biomol. NMR 6 (1995) 135–140.
[88] W.T. Franks, K.D. Kloepper, B.J. Wylie, C.M. Rienstra, Four-dimensional heteronuclear correlation experiments for chemical shift assignment of solid proteins, J. Biomol. NMR 39 (2007) 107–131.
[89] S. Hediger, B.H. Meier, R.R. Ernst, Adiabatic passage Hartmann-Hahn cross-polarization in NMR under magic-angle sample-spinning, Chem. Phys. Lett. 240 (1995) 449–456.